Brazilian Journal of Geophysics (2021) 39(4): 465-477
© 2021 Brazilian Geophysical Society
ISSN 0102-261X
DOI: 10.22564/rbgf.v39i4.2124

P- AND S-WAVE 3D VELOCITY MODELS FOR THE SOUTH AMERICAN PLATFORM

Carolina Rivadeneyra-Vera[1]*, Yvonne Font[2] and Marcelo B. Bianchi[1]

ABSTRACT. With the installation and growth of the Brazilian Seismographic Network (RSBR) since 2011, it is now possible to detect and locate events with magnitudes lower than 3.5 mb for Brazil, and better study the local and regional seismicity. Nevertheless, most of these events are located using 1D velocity models that lead to larger uncertainties precluding any correlation with the known geological structures. The use of heterogeneous 3D velocity models better predicts the travel times and guarantees the accuracy of hypocenter location; however, there is not yet a calibrated 3D velocity model for the South American Platform (SAP). In this study, integrating multiple local and regional geological and geophysical knowledge and average velocities of the crust and mantle, we have elaborated 3D P- and S-wave velocity models for the SAP, including the Central Andes area (down to 900 km). We tested the model locating the well-known 1998 Andean Aiquile earthquake (Bolivia), 6.6 Mw, obtaining successful results when compared with its ground truth location. We also satisfactorily located two other recent important events of the SAP, using local and regional body wave arrivals recorded by the RSBR. Finally, S-wave arrivals of near stations helped to constrain the event depths to expected values.

Keywords: heterogeneous velocity model, Brazilian seismicity; hypocenter location; NonLinLoc.

RESUMO. Em decorrência da implantação da Rede Sismográfica Brasileira (RSBR) em 2011, tornou-se possível detectar e localizar eventos com magnitudes menores de 3,5 mb no Brasil e aprofundar o estudo da sismicidade local e regional. Porém, a maioria desses eventos são localizados utilizando-se modelos de velocidade 1D, resultando em incertezas que não permitem correlacionar os hipocentros com as estruturas geológicas conhecidas. Em contrapartida, o uso de modelos 3D de velocidade prediz melhor os tempos de percurso das ondas e garante precisão na localização de hipocentros; porém, ainda não haviam sido desenvolvidos modelos 3D calibrados para a plataforma Sul-Americana. No presente estudo, integrando-se informações geológica e geofísica, local e regional, e velocidades médias da crosta e manto foram elaborados modelos 3D de velocidade das ondas P e S para a Plataforma Sul-americana e para os Andes Centrais (até 900 km de profundidade). Para testar a confiabilidade dos modelos, foi localizado o evento andino de Aiquile 1998, 6,6 Mw (Bolívia) usando-se chegadas regionais da onda P, com resultados compatíveis com o melhor epicentro conhecido. Também foram localizados satisfatoriamente dois outros eventos importantes. Finalmente, o uso de leituras da onda S de estações próximas restringe a profundidade hipocentral para valores esperados em cada caso.

Palavras-chave: modelo de velocidade heterogêneo; sismicidade brasileira; localização de hipocentros, NonLinLoc.

*Corresponding author: Carolina Rivadeneyra-Vera

[1]Universidade de São Paulo – USP, Dept. of Geophysics, Institute of Astronomy, Geophysics and Atmospheric Sciences - IAG, São Paulo, SP, 05508-090, Brazil – E-mails: carolina.vera@iag.usp.br, m.bianchi@iag.usp.br
[2]Université de la Côte d'Azur, IRD, CNRS, Observatoire de la Côte d'Azur, Géoazur, 250 Rue Albert Einstein, Sophia-Antipolis 06560 Valbonne, France – E-mail: font@geoazur.unice.fr

INTRODUCTION

Despite more than 90% of the global seismicity being located in the borders of the tectonic plates, the central Andean region and the stable part of South America also present an important seismic activity. Yearly in Brazil, it is observed at least two events of magnitude 4.0 mb and it is expected one of magnitude 5.0 mb each five years (Bianchi et al., 2018). Most of these earthquakes are regionally located using 1D standard velocity models (IASP91, AK135), showing larger uncertainties that do not permit any kind of correlation with the known local geological structures. Another model routinely used by the University of São Paulo Seismological Center (USP) in the context of the RSBR for local and regional events of major significance in Brazil is the 1D NewBR model, which tries to mimic regional travel times (Assumpção et al., 2010).

The use of 3D velocity models significantly improves the earthquake location in regional scale, since they capture the velocity heterogeneities of the crust and upper mantle and better predict the travel times; whose error prediction at regional scale when using 1D velocity models could exceed 8 seconds (Myers et al., 2010). Despite the advantage of using 3D velocity models to accurately locate regional and local earthquakes, the travel time calculation is straightforward for 1D velocity models, which makes it more convenient for monitoring systems. However, 3D velocity models have been successfully used to locate regional and local seismicity (Font et al., 2003; Wu et al., 2008; Lin, 2013; Nugraha et al., 2018).

Myers et al. (2010) developed the global 3D RSTT (Regional Seismic Travel Time) model that considers the effects of the crust and upper mantle structure to calculate the travel times for the regional waves that travel as head waves below the Moho (Pn). At regional distances, head wave arrival times are frequently used to locate regional earthquakes. For Eurasia and North Africa, model calibration improves epicenter accuracies of 5 km or more, when stations with a maximum distance of 15° (~1660 km) are considered. In South America, the 3D RSTT model and the iLoc algorithm (Bondár and Storchak, 2011) were used to locate the 1998 Andean Aiquile earthquake. The initial results so far obtained were not satisfactory since the epicenter determinations are more than ~20 km (the order of teleseismic location uncertainty) away from the rupture fault length determined using inSAR interferometry (Funning et al., 2005). The large difference between the well-known epicenter and the solutions using the 3D RSTT model was expected to occur due to the lack of a proper calibration of Pn travel times in South America. Those calibration values should be derived from ground truth events (GT5) that are scarce in the stable continental area of South America.

Figure 1 shows the epicenters given by international agencies, the one obtained using a standard 1D velocity model, the ones obtained using the 3D RSTT velocity model, and the rupture fault length determined by Funning et al. (2005). Even that the event was not totally correct using the RSTT model, it shows an improved epicenter when compared to the solution without any correction.

With the goal of improving earthquake location, we built P- and S-wave heterogeneous velocity models for the stable region of South America and Central Andes region to better assess travel time estimates. We integrated structural information (topography, sediment basement and Moho depth) with velocity information for sediments, crystalline crust, Andean crust, and recent mantle 3D tomography results.

These models were tested relocating the well-known Aiquilie earthquake, and other two recent earthquakes occurred in the platform; using the NonLinLoc (NLLoc) routine developed by Lomax et al. (2009).

METHODS

The velocity models were constructed integrating the structural and seismic velocity knowledge of the crust and combining it with the mantle 3D velocity model known for South America (Ciardelli et al., 2022). Since regional 3D velocity models are

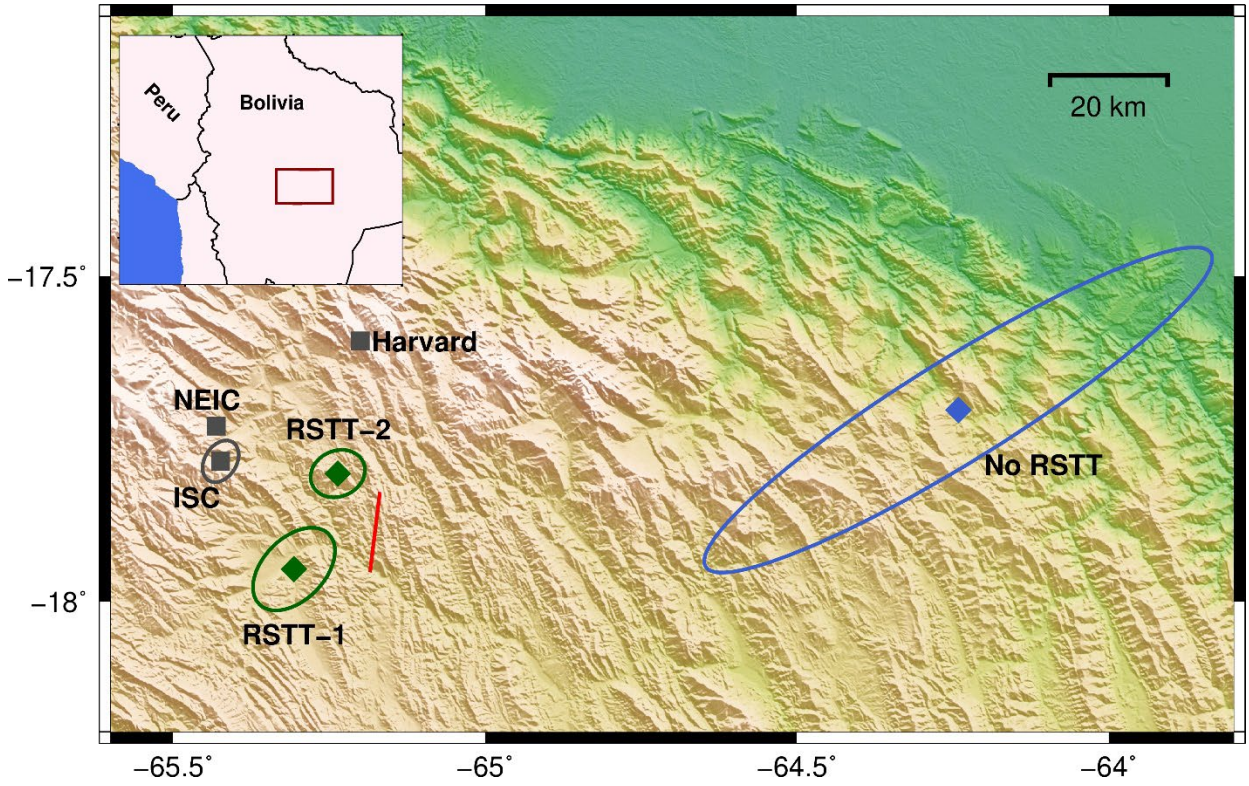

Figure 1 - Relocation of 1998 Aiquile earthquake (Bolivia) using the global 3D RSTT model (Myers et al., 2010). Red line: Fault rupture length determined by Funning et al. (2005). Gray squares: Epicenters given by different agencies (ISC, NEIC and Harvard). Blue diamond: Epicenter determined using stations up to 90° and 1D velocity model. RSTT-1: Epicenter determined with stations corrected with the 3D RSTT model up to 15°. RSTT-2: Epicenter determined with stations up to 90° and corrected with the 3D RSTT model up to 15°.

not available for our area of interest or do not have enough resolution in depth, we constructed velocity laws, that are the relationship between depth and wave's velocity, from already published relevant data for the sediments and crust.

Structural Data

We considered two first-order structures at the crustal-scale (sedimentary layer and the crystalline crust) that can be described by three interfaces:

1. Topography/bathymetry surface from the ETOPO1 model (NOAA National Geophysical Center, 2009). This is a 1-arc minute global relief model of the Earth's surface that integrates land topography and ocean bathymetry. In our study area, the topography varies from ~6 km above sea level in the Andean region to ~5 km below the sea level in the oceanic area.
2. Knowing the role of the sedimentary layer thickness in the process of epicentral location, we used the sediment information of the CRUST1.0 model (Laske et al., 2013) in most part of our study area. In the Paraná Basin it was used a local available grid of sediment thickness (personal communication).
3. The Moho is the most important discontinuity at the crustal-scale because of its high velocity contrast and relevant depth variations. We used the updated crustal thickness map of South America from Rivadeneyra-Vera et al. (2019).

Sedimentary and Crustal Velocities

To obtain the P-wave velocity laws, independently for sediments and crust, we compiled velocity information from the literature, giving preference to active seismic experiment data because of their controlled accurate parameters (time and position).

The predicted velocity laws were obtained from fitting a polynomial regression to the averages of the data collected.

To construct the velocity law for sediments (Fig. 2a), we used world data from sedimentary basins, since we had no easy access to the Brazilian regional scale data in a consistent manner. We collected data from Los Angeles Basin (Süss and Shaw, 2003), Indian Bengal Basin (Krishna and Rao, 2005; Damodara et al., 2017), Indian Palashi well (Murty et al., 2008), Norwegian-Danish Basin (Sandrin and Thybo, 2008), and Po Plain Basin in Italy (Molinari et al., 2015). The resulting velocity law varies between 1.7 km/s at the top of the sedimentary layer and 5.0 km/s at the bottom.

For the crystalline crustal velocity law, we considered two large different tectonic areas, the platform area that englobes all stable part of South America, and the Andean area that is a younger part of the continent. The boundary adopted between these two areas comes from the latest geological map of South America (CPRM, 2016), and also considering as Andean region, the area that presents a topography greater than 1500 meters above sea level.

Platform crust: it was collected Brazilian available data of the central part (Soares et al., 2018) and northeast region (Lima et al., 2019); also it was considered the average for platforms given by Christensen and Mooney (1995); and crustal velocity structures from the East European Craton (Starostenko et al., 2013), Siberian Craton (Cherepanova et al., 2013), China Craton (Wang et al., 2014), Chinese southern region (Zhu et al., 2018), Dominican Republic (Núñez et al., 2019), Eastern Piedmont, USA (Guo et al., 2019), and Cadiz Gulf (Lozano et al., 2020). The crustal velocity law obtained varies between 5.7 km/s and 7.1 km/s, without a vertical slope from 37 km downwards, and it is in concordance with the global average for platforms given by Christensen and Mooney (1995). The largest difference is the higher velocity at shallower depths up to 12 km observed in our predicted law. Nevertheless, the data available for Brazil (Soares et al., 2018; Lima et al., 2019) show higher velocities at shallower depths (Fig. 2b). All bibliography reviewed presents a similar pattern of velocity gradient; however, the crustal velocities at Cadiz Gulf and China Craton seem to be lower in approximately 1 km/s up to ~25 km, while Dominican Republic presents higher crustal velocities, being the Moho at shallower depth than it is in the other areas.

The Andean crust: considering the thicker crust under the Andes (up to ~70 km), and the different velocity gradient due to their tectonic evolution (Beck and Zandt, 2002), we calculated another velocity law for this region considering the global average for orogens given by Christensen and Mooney (1995), and also active seismic studies in the region (Beck and Zandt, 2002; Oncken et al., 2003; Chulick et al., 2013). The predicted velocity law (Fig. 2c) ranges from 5.7 km/s to 7.1 km/s, showing a higher gradient between 20 and 40 km depth, and does not vary significantly below 40 km depth. It also shows the low velocity zone between 10 km and 20 km depth found in previous works.

Figure 2d compares the two different velocity laws for the crystalline crust. From ~5 km down, the Andean velocity gradient is lower (light blue curve), meaning that at the same depth, crustal velocity in the Andes is lower than in the platform area. Low average crustal velocities are expected in the Andes, because of their felsic composition (Beck and Zandt, 2002). At the bottom of both velocity laws, the P-wave velocity reaches ~7.1 km/s that marks the transition to the Moho discontinuity. Also, it is important to remark that the velocity at the bottom of the sediments (~5 km/s) is lower than the velocity at the top of the crust (~5.8 km/s). This ensures a significant velocity increase in the transition from sediments to the crystalline crust.

For S-wave velocities, most of the studies consulted derive the S-wave velocity from P-wave models, adopting average values of Vp/Vs for each structure (sediments and crystalline crust). So, we opted for using the empirical relations proposed by Brocher (2005) between P- and S-wave velocities, which derive from a large dataset of seismic tomography, borehole's information, vertical seismic profile and laboratory measurements, to

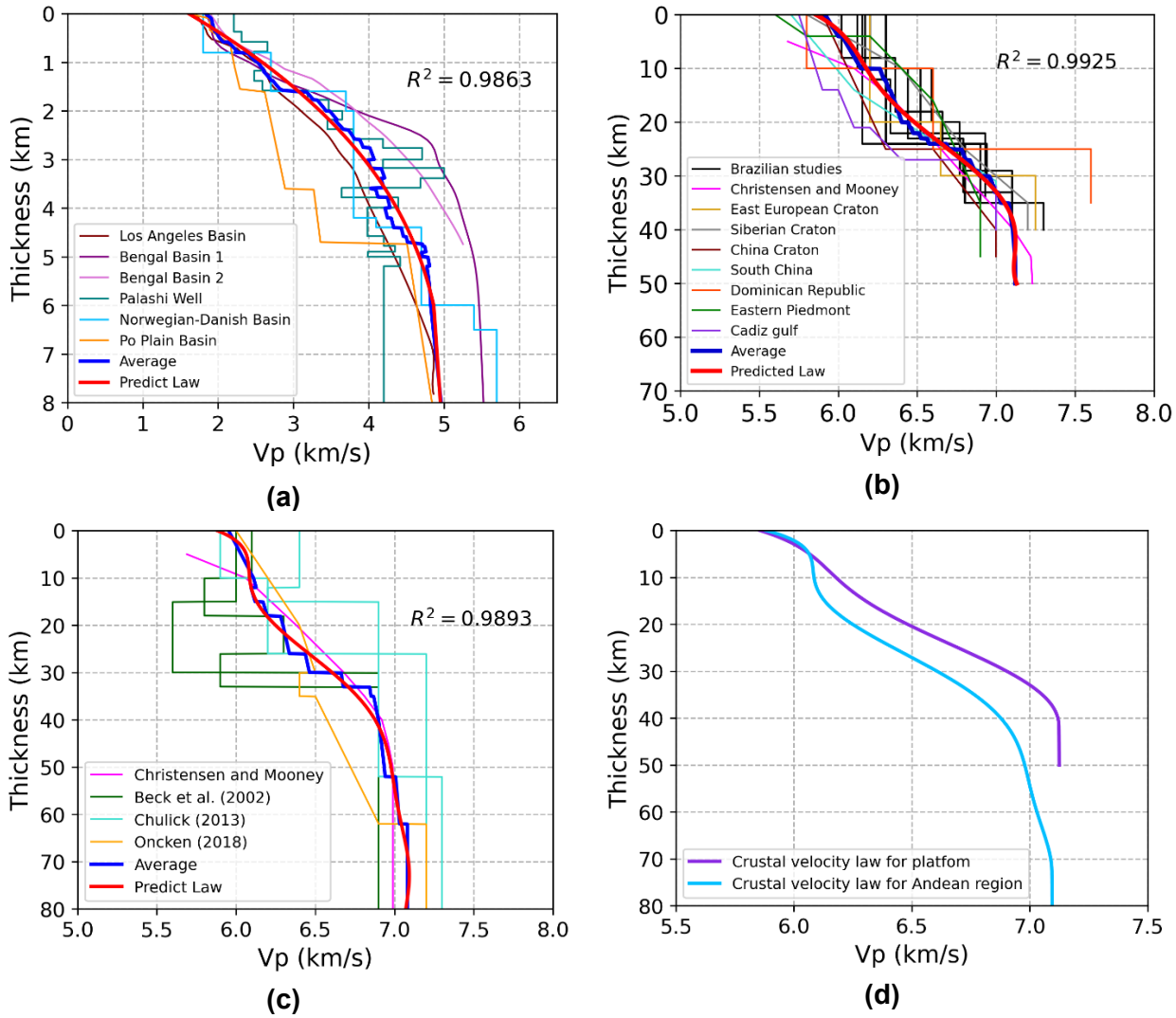

Figure 2 - P-wave velocity laws for (a) the sediment layer, (b) platform crust and (c) Andean crust. The references are given in the text. The blue line is the average velocity from the data collected, and the red curve is the polynomial regression that adjusts the blue line. (d) Comparison between velocity laws for the platform and the Andean region.

calculate S-wave velocity laws of each structure from the P-wave velocity laws discussed before.

Mantle Velocities

For the mantle velocity model, we used the SAAM23 3D P- and S-wave model for South America (Ciardelli et al., 2022), which is heterogeneously distributed with a horizontal resolution of 0.5°. It is consistent with the global discontinuities at ~410 and ~660 km depth (Kennett and Engdahl, 1991); and most important, with the position of the Nazca slab under the Andean and Sub-Andean region, according to Portner et al. (2020). We sampled the mantle velocities and adjusted the sample at the upper mantle position in our model, respecting the geographical position. The lowest mantle velocity is ~7.7 km/s, mainly under the oceanic area, and the highest crustal velocity (right above the Moho) is ~7.1 km/s which ensures a consistent velocity jump at the Moho discontinuity.

Parametrization and Model Construction

The model starts at 7 km above sea level and extends up to 900 km deep, considering that, for regional distances (up to 30°), the theoretical raypaths, that are the way that the waves follow considering a IASP91 velocity model (Kennett and Engdahl, 1991), do not go deeper than ~850 km, even for hypocenters deeper than 600 km (as the deep Andean earthquakes).

Considering the resolution of the available data, and the depth of our model, we defined a horizontal discretization of 0.5°x0.5° in latitude and longitude, while the vertical discretization assumes different values depending on the depth intervals being considered: shallower than 10 km depth, it is sampled every 1 km due to the higher velocity gradient of the sediment velocity law; between 10 and 50 km, the model is sampled every 2 km; and finally at mantle depths, every 5 km.

The volume of interest (from 75°W to 34°W and from 32°S to 10°N down to 900 km depth) was divided into blocks of the size previously defined resulting in 1 467 440 blocks. Each block is related to a velocity node used to represent the average velocity of the column below. Air and water velocity nodes are set to 0.3 km/s for P- and S-wave. Below the topography surface, each node was filled according to the structural information and the velocity laws obtained before. When one of the considered discontinuities (sediment basement or Moho depth) was between two nodes, the velocities of the two structure types were averaged.

For the transition area between the South American platform and the Andean region, and in order to smooth the velocity change, we also weighted the node velocities by considering the E-W distance between the nodes in each domain.

RESULTS

Figure 3 shows examples of vertical cross-sections taken at 30°S from the P-wave model. There is a clear velocity difference between the sediment layer, the crust, and the mantle. The lateral velocity variation in the crust depends on the thickness of the lithospheric structures (sedimentary basins, Moho depth and the distance to the Andean area). In the oceanic areas, the mantle velocities are slightly lower than in the continental areas. The black points represent the nodes with velocities of 0.3 km/s as discussed before. The Andean region, characterized by a high topography and a deeper Moho, has a slightly lower velocity compared with the platform area, at the same depth.

Figure 4 shows three horizontal slices, at 4, 38 and 100 km depth, for the P-wave and S-wave model. At 4 km depth, most of the continental area presents a crustal velocity, ~6.0 km/s for P-wave and ~3.5 km/s for S-wave, while there are still noticeable lower sediment velocities in the Paraná Basin. As expected, the ocean region presents velocities corresponding to the sedimentary layer, being higher in areas closer to the continent. The horizontal slice at 38 km depth shows mainly crustal velocities in the continent; besides, the Sub-Andean and Pantanal Basin regions present mantle velocities, since these areas have a thinner crust (Rivadeneyra-Vera et al., 2019). At 100 km depth, it is noticeable a different P- and S-wave velocity between the stable part of the continents and the younger Andes area, being evident the lower velocities in the Andean mantle, and a higher velocity below the cratonic areas.

Earthquake Locations

To assess the effect of the 3D velocity models on the determination of the earthquake position, we used the NonLinLoc routine (NLLoc) (Lomax et al., 2009) that has been used satisfactorily in regional and local locations using 3D velocity models (Béthoux et al., 2016; Lomax, 2020) with well-known events. The NLLoc uses an efficient global sampling algorithm to obtain the a-posteriori probability density function (PDF) over possible solutions, quantifying the agreement between predicted and observed arrival times to all uncertainties, forming a complete probabilistic solution (Lomax et al., 2009). The NLLoc also returns an expected solution that is the traditional best data misfit (lower RMS).

Andean Aiquile earthquake

Using our constructed velocity models and the NLLoc routine, we satisfactorily located the well-known Aiquile event using 14 P-wave arrivals, mostly belonging to the Bolivian network, located mainly in the Andean region. Figure 5 shows the relocation results; the semi-major axis of the error ellipsoid is about ~20 km, due to the fewer number

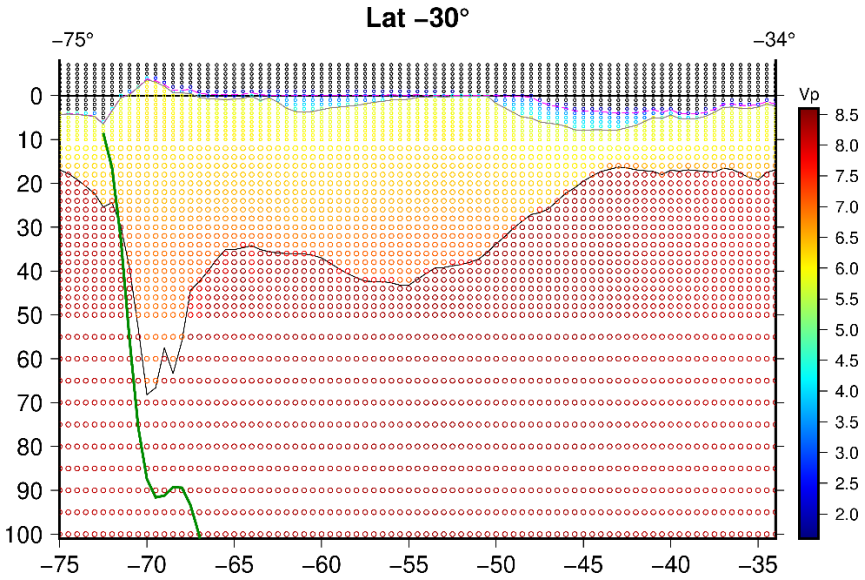

Figure 3 - Vertical cross-section at 30°S latitude, from 7km above the sea level to 100 km depth. Pink line: Topography surface. Gray line: Sediment basement. Black line: Moho discontinuity. Green line: Nazca Slab. The references are in the text. The black circles represent the air velocity nodes.

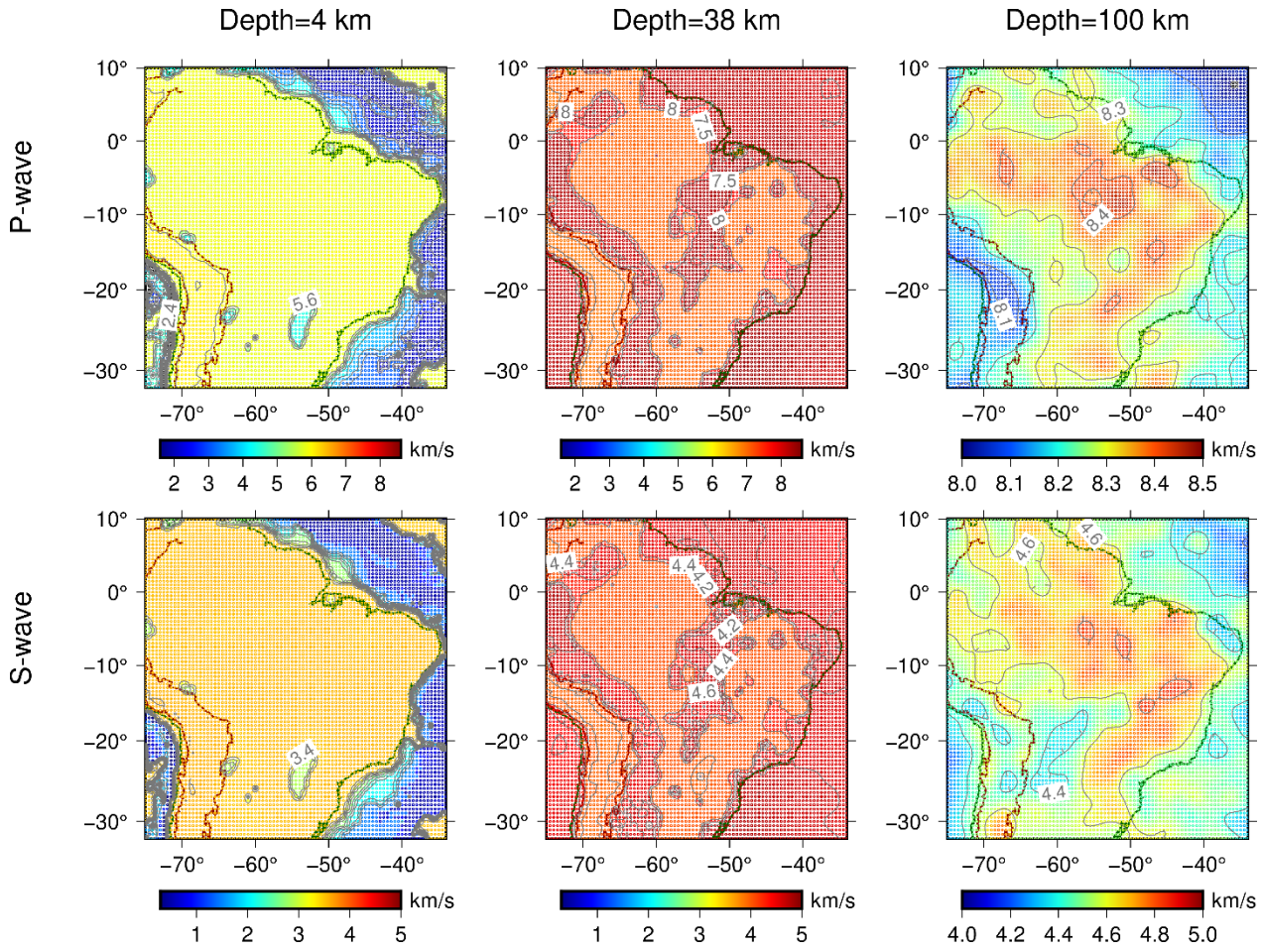

Figure 4 - Horizontal slices at 4,38 and 100km depth for P- and S-wave 3D velocity models. Red line: Andes limits. Green line: Continent-ocean margin. Grey lines: Velocity isolines.

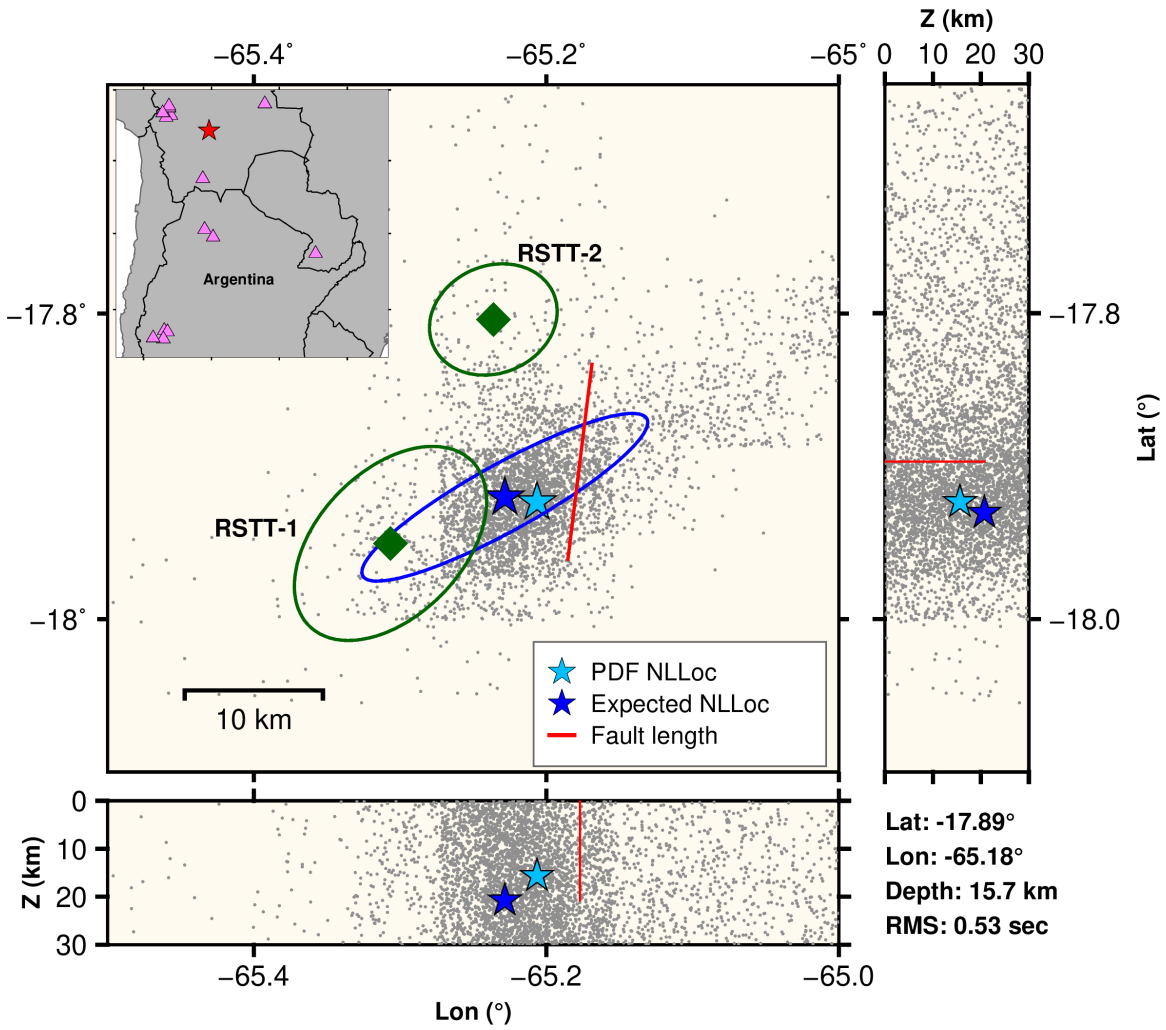

Figure 5 - Aiquile earthquake determinations using NLLoc routine and the 3D velocity model (blue and light blue stars). Red line: Rupture fault length (Funning et al., 2005). RSTT-1: Epicenter determined with stations up to 90° and corrected with RSTT model up to 15°. RSTT-2: Epicenter determined with stations corrected with RSTT model up to 15°. The stations used are shown as pink triangles in the embedded picture.

of stations considered, being the closest one at ~4° away. Most of them are located to the west of the event, existing an important azimuthal gap to the east, and therefore a major error in this direction. Despite the large uncertainty, all stations considered have residuals less than 1 second, even the stations located in the Andean region that generally present higher residual values; the final RMS is 0.53 seconds. The obtained solution, using the proposed 3D model, is the closest one to the fault rupture length (red line in Fig. 6) determined by Funning et al. (2005). Also, each gray dot represents each possible prior PDF solution of the unknown parameters. Those solutions are used to estimate the uncertainty presented.

Platform earthquakes

We also located two recent important events that occurred in the South American stable platform. In both cases, our solution was satisfactory, showing a final RMS lower than 0.8 seconds when using stations up to 15°. The first event was the Amargosa 2020-08-30 10:44:28 UTC earthquake, located in the northeast Brazil with a magnitude of 4,2 mR. With the RSBR seismological records, two epicenter determinations were obtained, one using the NewBR model with the Hypo71 routine (green star in Fig. 6), and the other one, the standard solution of the USP/RSBR (black star) using the SeisComP3 (Helmholtz-Centre Potsdam, 2008) LocSAT locator with the IASP91

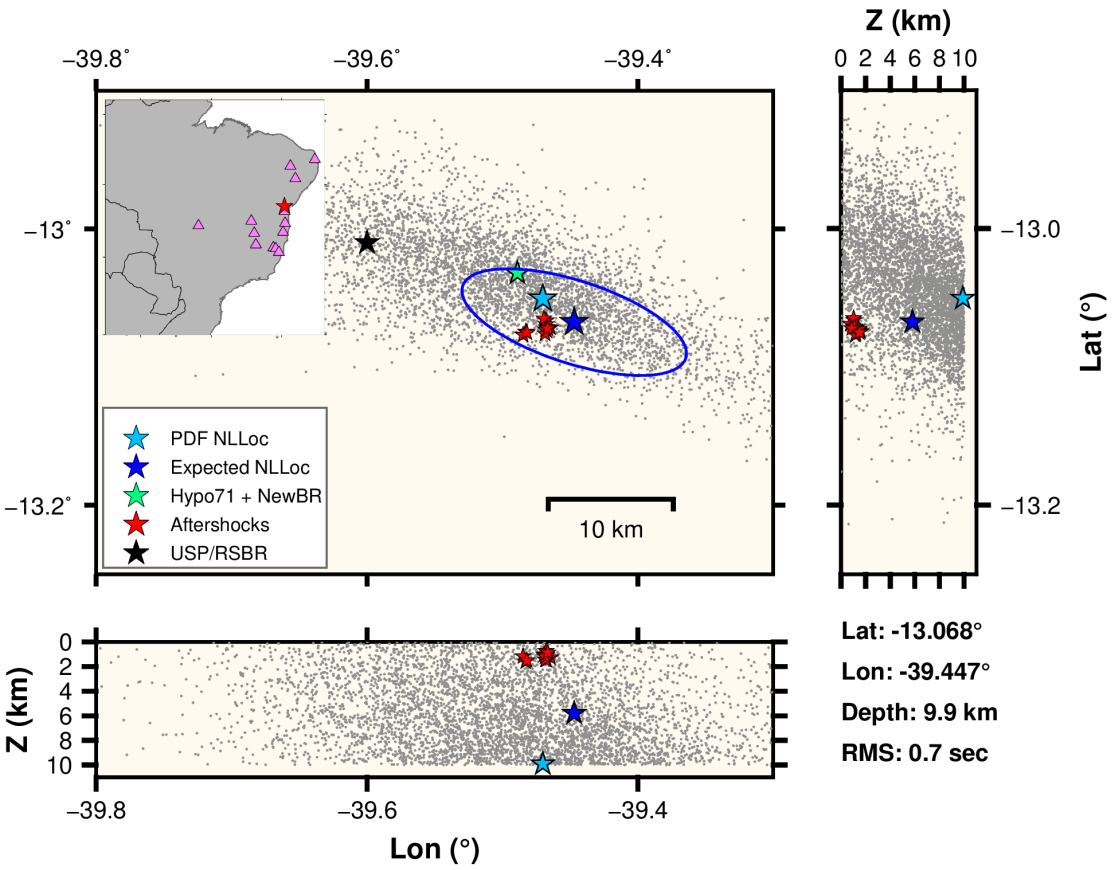

Figure 6 - Amargosa earthquake location using NLLoc routine and the 3D velocity models (blue and light blue stars). The red stars are aftershocks well located by a local network operated by the UFRN. Green star: Epicenter determined using the NewBR model and the Hypo71 routine. Black star: Epicenter given by the USP/RSBR using a 1D velocity model. The stations used are shown as pink triangles in the embedded picture.

model. This event had aftershocks well located, with uncertainties lower than 1 km (red stars), by a local network operated by the University of Rio Grande do Norte (UFRN), which were used as reference to qualify our solutions. To locate the event, we used 13 P-wave arrivals, being the closest at ~77km away and the farthest one at ~1300 km. We also used one S-wave arrival (from the closest station). Since it is a shallower earthquake, and the well-located aftershocks show depths less than 5 km, we restricted the NLLoc routine to search the hypocenter to the first 10 km depth (as shown in Fig. 6).

Used stations presented two azimuthal gaps, one in the NW direction in the continental part, and the other to the east, that corresponds to the oceanic area where there are no stations. Despite this configuration, we obtained a solution close to the reference area given by the aftershocks, with a RMS of 0,7 seconds, and uncertainties on the order of ~15 km (major axis of the error ellipse) in the direction of the azimuthal gaps commented before. Our restricted search from 0 to 10 km indicated a minimum RMS solution at ~5 km depth, deeper than the depth of 3 km estimated for the aftershocks by the local network. When looking to the depth of a prior PDF solution, there is a tendency to concentrate the solution at the 10 km limit.

The last performed test was done using readings from the very recent Guyana 2021-01-31 19:05:13 UTC earthquake (Fig. 7). This was the largest event (Mag. 5.7 mb) in the South American platform recorded by the RSBR so far (Bianchi et al., 2021). The USP Seismological Center located this event using regional stations and a 1D velocity model (black star in Fig. 7). The epicenter position was accurately determined using InSAR (red star, personal communication) and the local network studied by Bianchi et al. (2021). After the mainshock, a local network was installed, and it

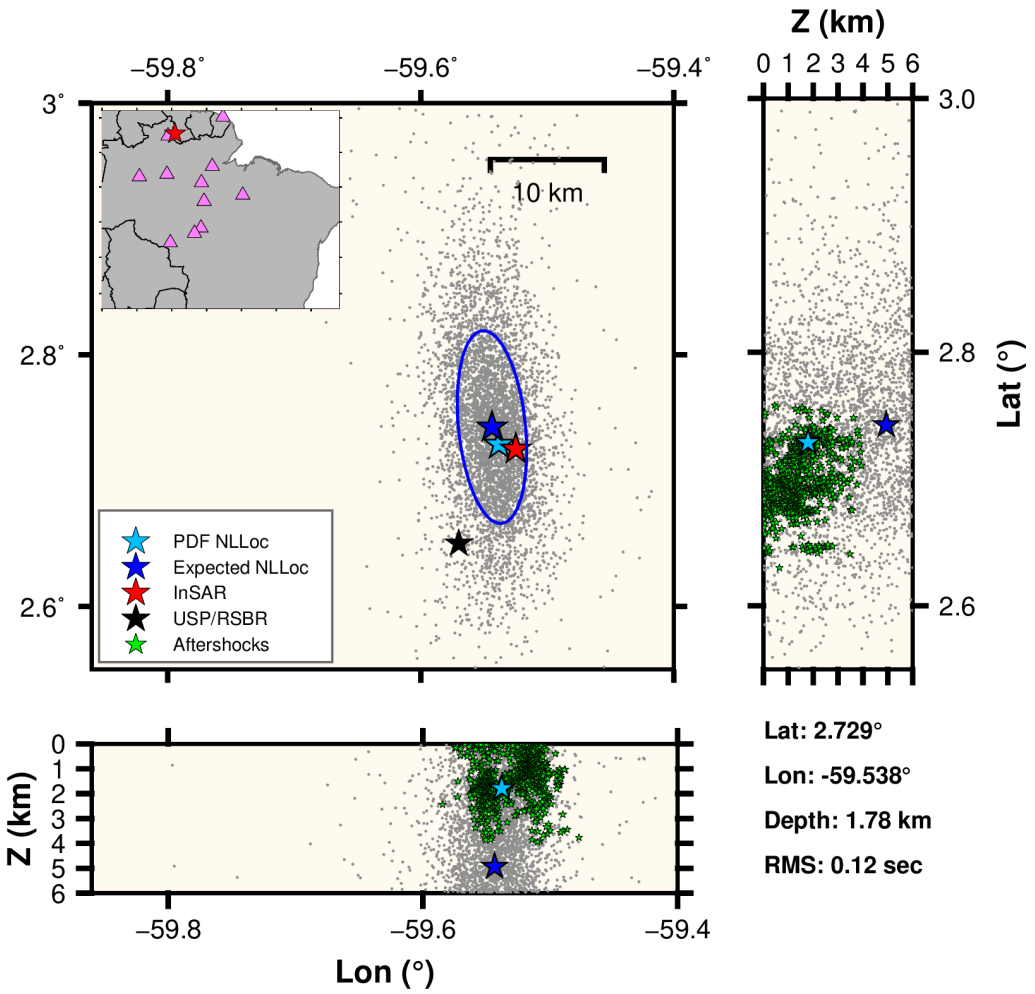

Figure 7 - Guyana earthquake relocation using NLLoc routine (blue and light blue stars). The red star is the best epicenter given by InSAR (personal communication). Black star: USP/RSBR solution. Green stars: The aftershock well located with a local network. The stations used are shown as pink triangles in the embedded picture.

recorded a well-located series of ~851 aftershocks with depths less than 4 km (Bianchi et al., 2021), that helped us to restrict the search of the best hypocenter in our tests.

In this case, we used 10 P-wave arrivals being the closest one at ~100 km, and the farthest at ~900 km; also, we used two S-wave arrivals (the closest ones). As the event occurred in the limit of Brazil and the Guyana, there is no available RSBR stations to the north; however, it was possible to use one international station from the French Guyana (network G, station MPG). Nevertheless, there is an important azimuthal gap to the north that led to a larger uncertainty in the north-south direction. Again, our solution is close to the best epicenter (InSAR), and within the uncertainty given by the determined PDF (blue ellipse).

CONCLUSIONS

In this study we constructed regional 3D velocity models that extend from 75°W to 34°W and from 32°S to 10°N, down to 900 km depth, for P- and S-wave that show a realistic velocity variation incorporating important lithospheric interfaces, such as sedimentary basement, Moho depths, the Nazca slab (when it is pertinent), and the global mantle discontinuities at ~410 and ~660 km.

Using our 3D velocity models, we successfully located the well-known Aiquile earthquake, as well as two events recorded on the platform by RSBR: the 2020 Amargosa event and the 2021 Guyana earthquake. Despite the important azimuthal gaps in the stations used, our solutions are coherent with the bench marks that we have (fault rupture length and local aftershock determinations) and in

all cases the best epicenter known is within our uncertainties.

The use of a S-wave counterpart 3D velocity model helps to constraint the depth solutions when using the closest stations. Unfortunately, no well settled ground truth event was recorded by the RSBR so far. The recent Guyana earthquake is under study by the USP/RSBR seismological group and it is a candidate to be the 1st GT event well recorded by the RSBR.

Finally, we made an invitation to all the community to test our model by making available a database with a computed model ready to be used with the NonLinLoc routine (10.5281/zenodo.6370310). The database includes the control configuration files, velocity grids and instructions for a straightforward application of the developed model.

ACKNOWLEDGMENTS

The authors would like to thank the support from the CNPq agency for the scholarship of C.R.V, and the support of the FUSP (Fundação de Apoio à Universidade de São Paulo) and Institute of Astronomy, Geophysics and Atmospheric Sciences (IAG/USP) for the financial support to develop most of this work at the Géoazur Laboratory in France.

REFERENCES

ASSUMPÇÃO M, ARDITO J & BARBOSA JR. 2010. An improved velocity model for regional epicentre determination in Brazil. In: IV Simpósio Brasileiro de Geofísica. Brasília, DF, Brazil: SBGf. 2010, p. cp

BECK S & ZANDT G. 2002. The nature of orogenic crust in the central Andes. Journal of Geophysical Research: Solid Earth, 107(B10), ESE-7. DOI: 10.1029/2000JB000124.

BÉTHOUX N, THEUNISSEN T, BESLIER MO, FONT Y, THOUVENOT F, DESSA JX, SIMON S, COURRIOUX G & GUILLEN A. 2016. Earthquake relocation using a 3D a-priori geological velocity model from the western Alps to Corsica: Implication for seismic hazard, Tectonophysics, vol. 670, p. 82-100. DOI: 10.1016/j.tecto.2015.12.016.

BIANCHI MB, ASSUMPÇÃO M, ROCHA MP, CARVALHO JM, AZEVEDO PA, FONTES SL, DIAS FL, FERREIRA JM, NASCIMENTO AF, FERREIRA MV & COSTA IS. 2018. The Brazilian Seismographic Network (RSBR): Improving Seismic Monitoring in Brazil. Seismological Research Letters, 89(2A), 452-457. DOI: 10.1785/0220170227.

BIANCHI MB, AMARAL C, CALHAU J, ROSA D, BAKSH J, ASSING D, BASDEO C, BRASILIO E, COLLAÇO B & ASSUMPÇÃO M. 2021. Automatic detection and quantification of earthquake locations and basin source parameter of the Guyana M5,7 2021 earthquake sequence. In: 4th Brazilian Seismology Symposium. 17th International Congress of the Brazilian Geophysical Society and EXPOGEf. Brazil: SBGf.

BONDÁR I & STORCHAK D. 2011. Improved location procedures at the International Seismological Centre. Geophysical Journal International, 186, 1220-1244. DOI: 10.1111/j.1365-246X.2011.05107.x.

BROCHER TM. 2005. Empirical relations between elastic wavespeeds and density in the Earth's crust. Bulletin of the seismological Society of America, 95(6), 2081-2092. DOI: 10.1785/0120050077.

CHEREPANOVA Y, ARTEMIEVA IM, THYBO H & CHEMIA Z. 2013. Crustal structure of the Siberian craton and the West Siberian basin: An appraisal of existing seismic data. Tectonophysics, 609, 154-183. DOI: 10.1016/j.tecto.2013.05.004.

CHRISTENSEN NI & MOONEY WD. 1995. Seismic velocity structure and composition of the continental crust: A global view. Journal of Geophysical Research: Solid Earth, 100(B6), 9761-9788. DOI: 10.1029/95JB00259.

CHULICK GS, DETWEILER S & MOONEY WD. 2013. Seismic structure of the crust and uppermost mantle of South America and surrounding oceanic basins. Journal of South American Earth Sciences, 42, 260-276. DOI: 10.1016/j.jsames.2012.06.002.

CIARDELLI C, ASSUMPÇÃO M, BOZDAĞ E, PETER D & VAN DER LEE, S. 2022. Adjoint Tomography of South America. Journal of Geophysical Research: Solid Earth, 127(2): e2021JB022575. DOI: 10.1029/2021JB022575.

CPRM. 2016. Tectonic map of South America, 2nd ed., scale 1:5,000,000. Commission for the Geological Map of the World, published by CPRM (Brazilian Geological Survey).

DAMODARA N, RAO VV, SAIN K, PRASAD A & MURTY A. 2017. Basement configuration of the West Bengal sedimentary basin, India as revealed by seismic refraction tomography: its tectonic implications. Geophysical Journal International, 208(3), 1490-1507. DOI: 10.1093/gji/ggw461.

FONT Y, KAO H, LIU CS & CHIAO LY. 2003. A comprehensive 3D seismic velocity model for the eastern Taiwan southernmost Ryukyu regions. Terrestrial Atmospheric and Oceanic Sciences, 14(2), 159-182.

FUNNING GJ, BARKE RM, LAMB SH, MINAYA E, PARSONS B & WRIGHT TJ. 2005. The 1998 Aiquile, Bolivia earthquake: A seismically active fault revealed with InSAR. Earth and Planetary Science Letters, 232(1-2), 39-49. DOI: 10.1016/j.epsl.2005.01.013.

GUO W, ZHAO S, WANG F, YANG Z, JIA S & LIU Z. 2019. Crustal structure of the eastern Piedmont and Atlantic coastal plain in North Carolina and Virginia, eastern North American margin. Earth, Planets and Space, 71(1), 1-22. DOI: 10.1186/s40623-019-1049-z.

HELMHOLTZ-CENTRE POTSDAM - GFZ GERMAN RESEARCH CENTRE FOR GEOSCIENCES AND GEMPA GmbH. 2008. The SeisComP seismological software package. GFZ Data Services. DOI: 10.5880/GFZ.2.4.2020.003.

KENNETT BLN & ENGDAHL E. 1991. Traveltimes for global earthquake location and phases identification. Geophysical Journal International, 105: 429-465. DOI: 10.1111/j.1365-246X.1991.tb06724.x.

KRISHNA V & RAO VV. 2005. Processing and modelling of short-offset seismic refraction coincident deep seismic reflection data sets in sedimentary basins: an approach for exploring the underlying deep crustal structures. Geophysical Journal International, 163(3), 1112-1122. DOI: 10.1111/j.1365-246X.2005.02792.x.

LASKE G, MASTERS G, MA Z & Pasyanos M. 2013. Update on CRUST1.0 A 1-degree global model of Earth's crust. In: Geophys. Res. Abstracts. vol. 15, p. 2658. Available on: <https://igppweb.ucsd.edu/~gabi/crust1/laske-egu13-crust1.pdf>.

LIMA MVA, STEPHENSON RA, SOARES JEP, FUCK RA, DE ARAÚJO VC, LIMA FT & ROCHA FA. 2019. Characterization of crustal structure by comparing reflectivity patterns of wide-angle and near vertical seismic data from the Parnaíba Basin, Brazil. Geophysical Journal International, 218(3), 1652-1664. DOI: 10.1093/gji/ggz227.

LIN G. 2013. Three-Dimensional Seismic Velocity Structure and Precise Earthquake Relocations in the Salton Trough, Southern California. Bulletin of the Seismological Society of America, 103(5), 2694-2708. DOI: 10.1785/0120120286.

LOMAX A. 2020. Absolute Location of 2019 Ridgecrest Seismicity Reveals a Shallow Mw 7.1 Hypocenter, Migrating and Pulsing Mw 7.1 Foreshocks, and Duplex Mw 6.4 Ruptures. Bulletin of the Seismological Society of America, 110(4), 1845-1858. DOI: 10.1785/0120200006.

LOMAX A, MICHELINI A & CURTIS A. 2009. Earthquake location, Direct, Global-Search Methods. In MEYERS, R. A. (ed. in chief), Encyclopedia of Complexity and System Science. Springer. DOI: 10.1007/978-0-387-30440-3_150.

LOZANO L, CANTAVELLA JV & BARCO J. 2020. A new 3-D P-wave velocity model for the Gulf of Cadiz and adjacent areas derived from controlled-source seismic data: application to nonlinear probabilistic relocation of moderate earthquakes. Geophysical Journal International, 221(1), 1-19. DOI: 10.1093/gji/ggz562.

MOLINARI I, ARGNANI A, MORELLI A & BASINI P. 2015. Development and testing of a 3D seismic velocity model of the Po Plain sedimentary basin, Italy. Bulletin of the Seismological Society of America, 105(2A), 753-764. DOI: 10.1785/0120140204.

MURTY A, SAIN K & PRASAD BR. 2008. Velocity structure of the West-Bengal sedimentary basin, India along the Palashi-Kandi profile using a travel-time inversion of wide-angle seismic data and gravity modeling-an update. Pure and applied geophysics, 165(9), 1733-1750. DOI: 10.1007/s00024-008-0398-5.

MYERS S, BEGNAUD M, BALLARD S, PASYANOS M, PHILLIPS W, RAMIREZ A, ANTOLIK M, HUTCHENSON K, DWYER J,

ROWE C & WAGNER G. 2010. A Crust and Upper-Mantle Model of Eurasia and North Africa for Pn Travel-Time Calculation. Bulletin of the Seismological Society of America, 100, 640-656. DOI: 10.1785/0120090198.

NOAA NATIONAL GEOPHYSICAL CENTER. 2009. ETOPO1 1 arc-minute global relief model, Tech. Report., NOAA National Centers for Environmental Information. DOI: 10.7289/V5C8276M.

NUGRAHA AD, SHIDDIQI HA, WIDIYANTORO S, THURBER CH, PESICEK JD, ZHANG H, WIYONO SH, RAMDHAN M, WANDONO & IRSYAM M. 2018. Hypocenter Relocation along the Sunda Arc in Indonesia, Using a 3D Seismic-Velocity Model. Seismological Research Letters, 89(2A), 603-612. DOI: 10.1785/0220170107.

NÚÑEZ D, CÓRDOBA D & KISSLING E. 2019. Seismic structure of the crust in the western Dominican Republic, Tectonophysics, 773, 228,224. DOI: 10.1016/j.tecto.2019.228224.

ONCKEN O, ASCH G, HABERLAND C, METCHIE J, SOBOLEV S, STILLER M, YUAN X, BRASSE H, BUSKE S, GIESE P. 2003. Seismic imaging of a convergent continental margin and plateau in the central Andes (Andean Continental Research Project 1996 (ANCORP'96)). Journal of Geophysical Research: Solid Earth, 108(B7). DOI: 10.1029/2002JB001771.

PORTNER DE, RODRÍGUEZ EE, BECK S, ZANDT G, SCIRE A, ROCHA MP, BIANCHI MB, RUIZ M, FRANÇA GS, CONDORI C & ALVARADO P. 2020. Detailed Structure of the Subducted Nazca Slab into the Lower Mantle Derived from Continent-Scale Teleseismic P Wave Tomography. Journal of Geophysical Research: Solid Earth, 125(5), e2019JB017, 884. DOI: 10.1029/2019JB017884.

RIVADENEYRA-VERA C, BIANCHI M, ASSUMPÇÃO M, CEDRAZ V, JULIÀ J, RODRÍGUEZ M, SÁNCHEZ L, SÁNCHEZ G, LOPEZ-MURUA L, FERNANDEZ G, FUGARAZZO R & TEAM TBP. 2019. An Updated Crustal Thickness Map of Central South America Based on Receiver Function Measurements in the Region of the Chaco, Pantanal, and Paraná Basins, South-western Brazil, Journal of Geophysical Research: Solid Earth, 124(8), 8491-8505. DOI: 10.1029/2018JB016811.

SANDRIN A & THYBO H. 2008. Seismic constraints on a large mafic intrusion with implications for the subsidence history of the Danish Basin. Journal of Geophysical Research: Solid Earth, 113(B9). DOI: 10.1029/2007JB005067.

SOARES JE, STEPHENSON R, FUCK RA, LIMA MV, ARAÚJO VC, LIMA FT, ROCHA FA & TRINDADE CR. 2018. Structure of the crust and upper mantle beneath the Parnaíba Basin, Brazil, from wide-angle reflection–refraction data. Geological Society, London, Special Publications, 472(1), 67-82. DOI: 10.1144/SP472.9.

STAROSTENKO V, JANIK T, KOLOMIYETS K, CZUBA W, ŚRODA P, GRAD M, KOVÁCS I, STEPHENSON R, LYSYNCHUK D, THYBO H. 2013. Seismic velocity model of the crust and upper mantle along profile PANCAKE across the Carpathians between the Pannonian Basin and the East European Craton. Tectonophysics, 608, 1049-1072. DOI: 10.1016/j.tecto.2013.07.008.

SÜSS MP & SHAW JH. 2003. P-wave seismic velocity structure derived from sonic logs and industry reflection data in the Los Angeles basin, California. Journal of Geophysical Research: Solid Earth, 108(B3). DOI: 10.1029/2001JB001628.

WANG S, WANG F, ZHANG J, JIA S, ZHANG C, ZHAO J & LIU B. 2014. The P-wave velocity structure of the lithosphere of the North China Craton-Results from the Wendeng-Alxa Left Banner deep seismic sounding profile. Science China Earth Sciences, 57(9), 2053-2063. DOI: 10.1007/s11430-014-4903-7.

WU YM, CHANG CH, ZHAO L, TENG TL & NAKAMURA M. 2008. A Comprehensive Relocation of Earthquakes in Taiwan from 1991 to 2005. Bulletin of the Seismological Society of America, 98(3), 1471-1481. DOI: 10.1785/0120070166.

ZHU J, XU H, QIU X, YE C & LI S. 2018. Crustal structure and rifting of the northern South China Sea margin: Evidence from shoreline-crossing seismic investigations. Geological Journal, 53(5), 2065-2083. DOI: 10.1002/gj.3034.

C.R.-V.: Elaboration of the 3D velocity models and tests carried out. Elaboration of the manuscript and participation in the discussion of results. **Y.F.:** Participation as advisor in the elaboration of the models and discussion of results, and revision of the manuscript. **M.B.B.:** Contribution in the tests carried out, discussion of results and revision of the manuscript.

Received on December 31, 2021 / Accepted on May 6, 2022